

Electrochemical and structural analysis of a novel symmetrical bis-Schiff base with herringbone packing motif



Tomislav Balić, Berislav Marković, Martina Medvidović-Kosanović*

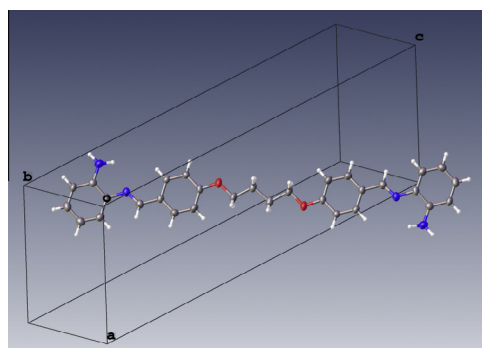
Department of Chemistry, University of Osijek, Cara Hadrijana 8A, HR-31 000 Osijek, Croatia

HIGHLIGHTS

- Symmetrical bis-Schiff base.
- X-ray, FTIR, NMR, elemental analysis, TG/DSC, voltammetry.
- Electrochemical analysis.
- Herringbone structural motif.

GRAPHICAL ABSTRACT

Crystal structure of the novel synthesized Schiff base, (1E)-1-N-[[4-(4-[(E)-N-(2-aminophenyl)carboxymidoyl]phenoxy)butoxy]phenyl]methylidene}benzene-1,2-diamine.



ARTICLE INFO

Article history:

Received 15 September 2014

Received in revised form 26 November 2014

Accepted 2 December 2014

Keywords:

Bis-Schiff base

Single crystal X-ray analysis

Herringbone packing motif

Electrochemistry

Voltammetry

ABSTRACT

A novel symmetrical bis-Schiff base was synthesized and characterized by means of single crystal X-ray diffraction, FT-IR and NMR spectroscopy, elemental, TG/DSC and electrochemical analysis. The synthesized molecule represents a rare example of symmetrical bis-Schiff base with uncondensed primary amino group as the final reaction product. The molecule is planar, with largest deviation of aminophenyl benzene ring from the plane calculated through the aliphatic chain in the amount of $4.93(1)^\circ$. In the crystal, the molecules are primarily linked by hydrogen bonds involving primary amino groups and weak C—H... π interactions. Consequently, these interactions are arranging molecules into herringbone packing motif. The FT-IR and NMR spectra indicated presence of both imino and amino groups in dissolved and solid state, therefore confirming consistency of the studied material and also molecular structure determined by X-ray diffraction. Electrochemical study has shown that the oxidation of the investigated Schiff base is irreversible, diffusion controlled process and that the oxidation products are adsorbed on the glassy carbon electrode surface.

© 2014 Elsevier B.V. All rights reserved.

Introduction

Symmetrical bis-Schiff bases have been widely studied due to their pronounced biological and pharmacological activity [1], optical [2], photochromical [3], thermochemical [4] properties and other outstanding material properties. Furthermore, they can

* Corresponding author. Tel.: +385 31 399 959; fax: +385 31 399 969.

E-mail address: mmkosano@kemija.unios.hr (M. Medvidović-Kosanović).

easily act as different types of polydentate ligands and, because of their diversified donor groups (or atoms), are suitable to be chelating agents. Complex compounds of Schiff bases are considered to be a transitional state between simple coordination compounds and metalloproteins [5]. Due to the presence of two distinct donor sites in bis-Schiff bases, they can be regarded as a promising ligands for preparation of bimetallic complexes [6]. Important work considering complex compounds with bis-Schiff bases containing primary amino group is reported in recent literature [7,8]. Symmetrical bis-Schiff bases were also studied as liquid crystalline materials [9–11]. Because of the presence of basic imino centers, optical properties of this compounds can be altered by changing acid–base balance [12]. Symmetrical bis-Schiff bases were also used in design of liquid crystal polymers or oligomers as a potential luminescent [13] and organic photovoltaic materials [14]. It has been recently pointed out that some compounds that exhibit herringbone packing motif are promising building blocks for preparation of organic thin-film transistors [15]. Among other factors, optical and electronic performances of these materials strongly depend upon crystal packing of molecules. Clearly, local packing of molecules in herringbone packing motif (herringbone angle, roll angle and interplanar distance) determinates degree of intermolecular orbital overlap which is important for charge transport inorganic thin-film transistors [16]. There are several examples of aromatic bis-Schiff bases that exhibit herringbone packing motif [17,18]. Straightforward synthesis of azomethines along with promising optical and electrochemical properties has pointed out these compounds as an interesting alternative for preparation of organic electronics [19].

In this study, a novel symmetrical bis-Schiff base (1E)-1-N-[[4-(4-((E)-N-(2-aminophenyl)carboxyimido)phenoxy)butoxy)phenyl]methylidene)benzene-1,2-diamine was synthesized. This molecule represents a rare example of a symmetrical bis-Schiff base with uncondensed primary amino group (there are only few known examples of similar structures [20,21]). The compound was characterized by means of single crystal X-ray diffraction, FT-IR spectroscopy, NMR spectroscopy, TG/DSC and elemental analysis. In addition, oxido-reduction properties of the synthesized compound have been studied. Preliminary information acquired from this study could be very useful as indicators for potential applications of title compound (i.e. organic semiconductor, liquid crystal, potentiometric sensor, etc.).

Experimental

Chemicals and apparatus

All commercially available chemicals were of reagent grade and used as purchased. Dialdehyde 4-[4-(4-formylphenoxy)butoxy]benzaldehyde was prepared by previously reported method [22]. All solvents were purchased commercially. N,N-dimethylformamide (DMF) was purchased from Fischer Chemical and lithium chloride (LiCl) from BDH Prolabo and were used without further purification.

FT-IR spectrum was recorded on a Shimadzu FTIR 8400S spectrophotometer using the DRS 8000 attachment, in the 4000–400 cm^{-1} region. The measured sample was diluted with IR grade KBr. Data collection and analysis were performed using Shimadzu IRsolution 1.3 program. Thermogravimetric analysis was performed using a simultaneous TGA/DSC analyser (Mettler-Toledo TGA/DSC 1). The compound was placed in aluminium pan (100 μL) and heated in nitrogen atmosphere (200 mL min^{-1}) up to 590 $^{\circ}\text{C}$ at a rate of 10 $^{\circ}\text{C min}^{-1}$. The data collection and analysis were performed using the program package STARE Software 10.0 [23]. C, H and N analyses were provided by the Analytical Services

Laboratory of the Ruđer Bošković Institute, Zagreb. The ^1H NMR and ^{13}C NMR were recorded on NMR (300 MHz) Bruker instrument using deuterated chloroform as solvent at NMR Laboratory of the Ruđer Bošković Institute, Zagreb.

X-ray diffraction data were collected at room temperature on an Oxford Diffraction Xcalibur 3 CCD diffractometer with graphite-monochromated Mo K_{α} radiation ($\lambda = 0.71073 \text{ \AA}$) using ω -scans. The crystal was glued to a thin glass needle. The data reduction was performed using the CrysAlis software package [24]. The structure was solved using SIR2004 [25]. Refinement and analysis of the structure were done using the programs integrated in the WinGX system [26]. The refinement procedure was performed using SHELXL-97 [27]. The non-hydrogen atoms were refined anisotropically. Hydrogen atoms in the structure were placed in calculated positions and refined using the riding model except amino hydrogen atoms that were located in differential Fourier map and refined freely. Geometrical calculations and molecular graphics were done using PLATON [28,29] and MERCURY [30]. The crystallographic data are summarized in Table 1.

Electrochemical experiments were performed on PalmSens potentiostat/galvanostat (PalmSens BV, Utrecht, The Netherlands) driven by PSTrace 4.2 software. A conventional three-electrode cell was used with a glassy carbon as a working electrode, non-aqueous Ag/Ag^+ as a reference electrode and a platinum wire as a counter electrode. The glassy carbon working electrode was polished with coarse diamond polish (1 μm , ALS, Japan) and with polishing $\alpha\text{-Al}_2\text{O}_3$ (0.05 μm , ALS, Japan) before each measurement. Cyclic voltammetry scan rate was 100 mV s^{-1} . The differential pulse voltammetry conditions were: scan increment 5 mV, pulse amplitude 25 mV, pulse width 70 ms and scan rate 5 mV s^{-1} .

Synthesis

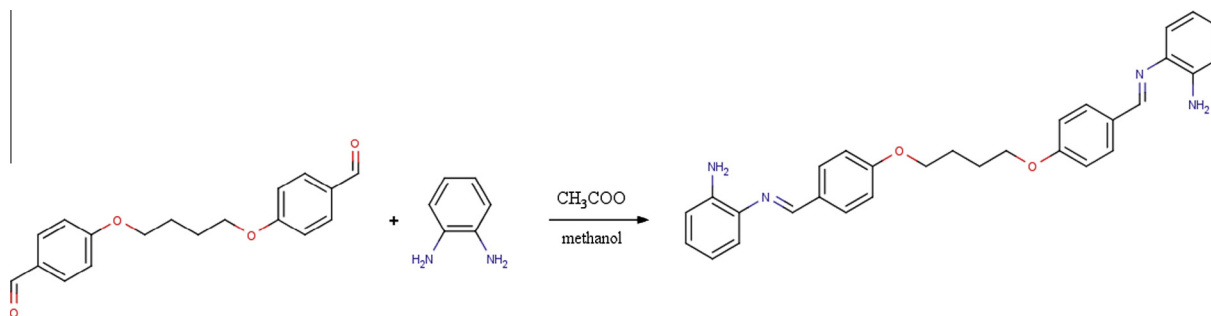
The synthetic pathway leading to the title compound is denoted in Scheme 1. Dialdehyde (0.6 g, 2 mmol) was dissolved in 40 ml of methanol and 2–3 drops of glacial acetic acid were added to this solution. The resulting solution was heated to reflux temperature on a water bath and 0.49 g (4.5 mmol) of o-phenylenediamine dissolved in 25 ml of methanol were gradually added. The mixture was heated at reflux temperature for 3 h. After the reaction was completed, mixture was left at room temperature for 24 h. The

Table 1
Crystallographic data and structure refinement details for title compound.

Empirical formula	$\text{C}_{30}\text{H}_{30}\text{N}_4\text{O}_2$
M_r	478.58
T (K)	294(2)
Crystal colour, habit	yellow, plate
Crystal size (mm^3)	$0.52 \times 0.35 \times 0.06$
Crystal system	orthorhombic
Space group	$P bca$
Unit cell parameters	
a (\AA)	10.1933(9)
b (\AA)	6.8890(6)
c (\AA)	35.214(3)
V (\AA^3)	2472.8(4)
Z	4
D_{calc} (g cm^{-3})	1.286
μ (mm^{-1})	0.082
$F(000)$	1016
Measured reflections	8674
Independent reflections	2425
Number of parameters	171
R_1^a , [$F_o \geq 4\sigma(F_o)$]	0.0577
wR_2^b	0.1044
Goodness of fit on F^2 , S	1.012
Largest diff. peak and hole ($e \text{ \AA}^{-3}$)	0.272 and -0.175

$$^a R = \sum ||F_o - |F_c|| / \sum |F_o|$$

$$^b wR = [\sum (F_o^2 - F_c^2)^2 / \sum w(F_o^2)^2]^{1/2}$$



Scheme 1. Synthetic pathway for the synthesis of the title compound.

Table 2

Selected interatomic bond distances (Å), bond angles (°) and torsion angles (°) for title compound.

Selected bond distances (Å)		Selected bond angles (°)		Selected torsion angles (°)	
C1–N1	1.373(3)	N2–C7–C8	123.0(2)	N1–C1–C6–N2	–3.4(3)
C6–N2	1.421(3)	O1–C14–C15	108.03(1)	O1–C14–C15–C15(i)	–177.6(2)
C7–N2	1.268(3)	C14–C15–C15(i)	110.9(3)	C15–C14–O1–C11	–178.62(1)
C11–O1	1.367(3)	C11–O1–C14	117.56(1)	C8–C7–N2–C6	–179.5(2)
C14–O1	1.428(3)	C7–N2–C6	120.7(2)		

(i) $-x + 1, -y, -z + 1$.

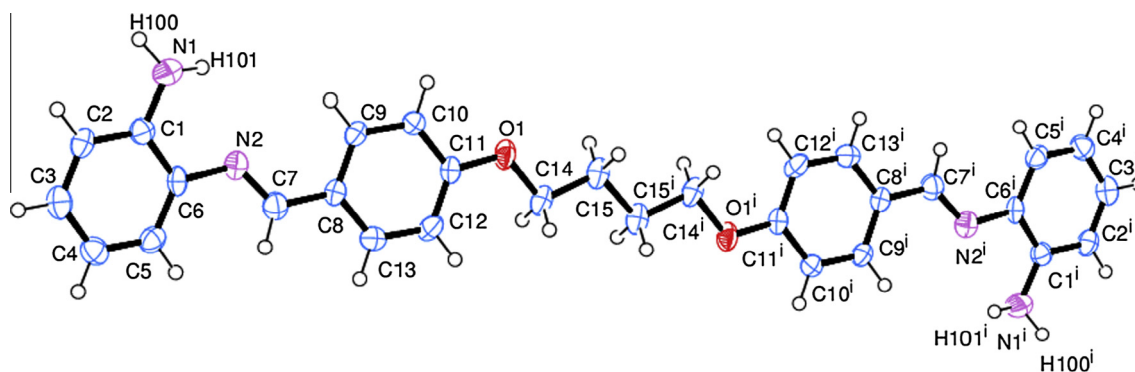


Fig. 1. The ORTEP diagram of the molecular structure of the title compound with atom numbering scheme. The thermal ellipsoids are drawn at the 50% probability level.

yellow crystalline product was filtered and washed with cold ethanol and diethyl ether. Crude product was recrystallized from benzene to yield pure product as yellow crystals. Suitable single crystals for X-ray diffraction experiments were obtained by slow evaporation from benzene solution. Yield: 82%. M.p. (DSC): 163 °C. Anal. Calc. for $C_{30}H_{30}N_4O_2$: C 75.29, H 6.32, N 11.71%. Found: C 74.44, H 6.58, N 9.98%.

Results and discussion

Characterization of compound

The IR spectrum of compound exhibits bands at 3450 and 3360 cm^{-1} due to $\nu(N-H)$ stretching vibration of the primary amino group. The vibrations at 2945–2874 cm^{-1} are due to aliphatic C–H stretching. The $\nu(N-H)$ stretching vibration (3450–3360 cm^{-1}) has lower values compared to those in *o*-phenylenediamine [31] and this can be explained by strong intramolecular interactions which involves primary amino group of compound. The C=N stretching vibration is coupled with C=C stretching vibration of aromatic ring and is located around 1600 cm^{-1} . Also, the spectrum exhibit strong vibration at 1248 cm^{-1} which is assigned to stretching of $C_{aromatic}-O-C_{aliphatic}$ group. The vibrations at 836 cm^{-1} and 743 cm^{-1} are assigned to

out-of-plane C–H bending vibrations of the para (C8–C13) and ortho (C1–C6) substituted benzene rings, respectively.

The 1H NMR spectrum of compound shows multiplet signals at 6.65–7.99 ppm due to aromatic protons. Methylene proton signals of aliphatic chain occur in the region between 1.90 ppm and 4.19 ppm. Signal for the imine protons appears at 8.47 ppm and for primary amine protons at 5.34 ppm. The ^{13}C NMR spectrum exhibits signals at 25.94 ppm and 67.62 ppm corresponding to methylene carbon. The aromatic carbons chemical shift signals are located in the interval from 114.66 ppm up to 157.01 ppm. The carbon atom of the imine group exhibits chemical shift at 161.48 ppm.

The TG curve of the compound shows two-step thermal decomposition. The first thermal event starts at 173 °C with experimental mass loss of 7.3% and could be related to thermal decomposition of primary amino groups (calc. 6.7%). The second thermal event is at 387 °C and can be related to thermal decomposition of compound. The DSC curve exhibits only one endothermic event at 165 °C that is assigned as the melting point of compound.

Crystal structure of title compound

The asymmetric unit comprises only one half of the molecule with crystallographic inversion centre lying in the centre of the

Table 3
Hydrogen bond geometry (Å, °) for title compound.

D—H...A	d(D—H)	d(H...A)	d(D...A)	∠(DHA)
C9—H9...N1(i)	0.95	2.84	3.268(3)	108.2
N1—H100...N2(ii)	0.95	2.52	3.312(3)	141
N1—H101...N1(iii)	0.994	2.279	2.698(3)	104
D—H...A	d(D—H)	d(H...Cg)	d(D...Cg)	∠(DHCg)
C(3)—H(3)...Cg1(iv)	0.95	2.75	3.600(3)	149
C15—H15B...Cg2(v)	0.99	2.88	3.775(3)	152

Symmetry codes used to generate equivalent atoms: (i) $-x + 1, -y, -z + 1$, (ii) $x + 1/2, y + 1/2, z$, (iii) x, y, z , (iv) $1 - x, 1/2 + y, 1/2 - z$, (v) $1 - x, 1 - y, 1 - z$.

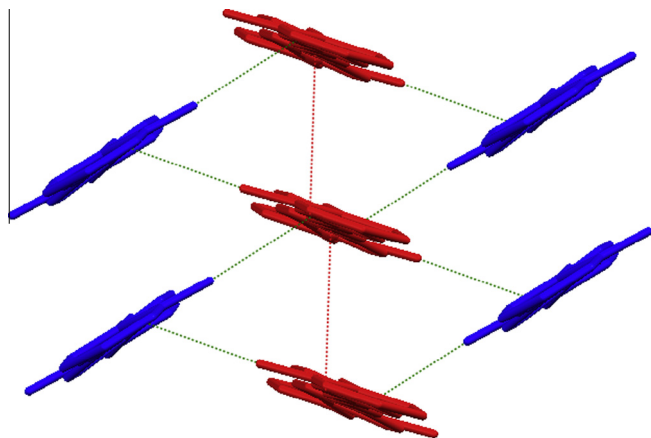


Fig. 2. View of the herringbone packing arrangement of the compound with the intermolecular N—H...N interactions (green dashed) and C—H... π interactions (red dashed). Hydrogen atoms are omitted for clarity. (For interpretation of the references to colour in this figure legend, the reader is referred to the web version of this article.)

molecule. Selected bond lengths, bond angles and torsion angles are listed in Table 2 and the molecular structure is shown in Fig. 1. The bond distances and angles are within the normal ranges and are in close agreement with literature values [32].

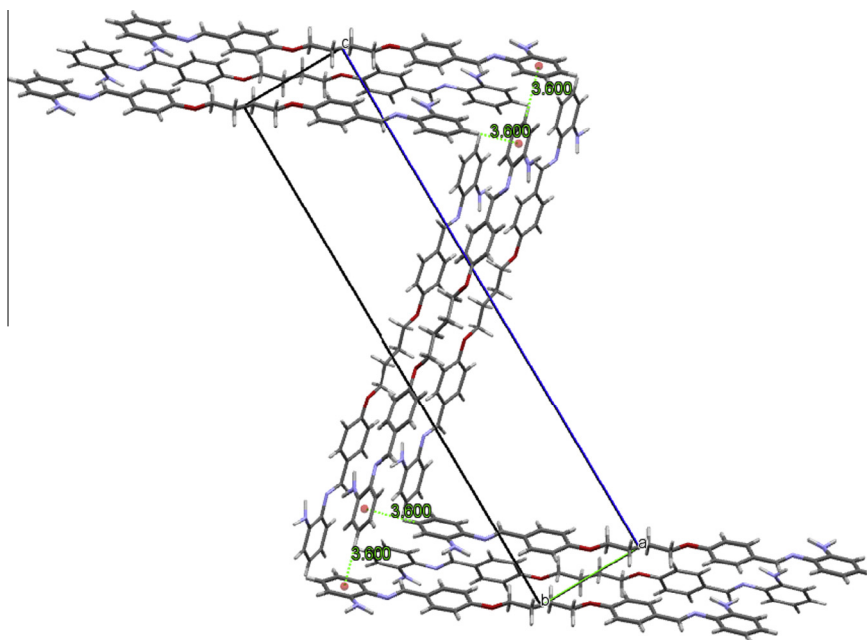


Fig. 3. Supramolecular staircase motif in the title compound with C3—H3... π interactions denoted (green dashed). (For interpretation of the references to colour in this figure legend, the reader is referred to the web version of this article.)

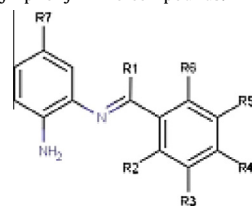
The molecule is essentially planar, the aminophenyl benzene ring is inclined to the plane calculated through the aliphatic chain only by $4.93(1)^\circ$. The two largest deviations of the atoms from the least-squares plane are $0.1518(1)$ Å and $0.129(2)$ Å of imino and amino nitrogen atoms, respectively. The aliphatic chain adopts all *trans* conformation, which consequently contributes to the planarity of the molecule. The molecule adopts (E)-conformation about imine N2—C7 bond with the torsion angle C8—C7—N2—C6 of $-179.5(2)^\circ$. Furthermore, the planarity of molecule is stabilized by a strong intramolecular hydrogen bond of the amino group and imino nitrogen atoms, N1—H101...N2 [$2.698(3)$ Å] (Table 3). A similar intramolecular interaction was observed in some semi-carbazones [33] and hydrazides [34]. In the crystal, the molecules are primarily linked through the terminal amino groups. Two neighbouring molecules are connected via an intermolecular N1—H100...N2 [$3.311(3)$ Å] hydrogen bond. The dihedral angle between these molecules is $54.14(1)^\circ$. In addition, parallel molecules are linked by weak C15—H15B... π [$3.775(3)$ Å] interactions (Fig. 2). The arrangement of the molecules in the crystal resembles a simple herringbone motif, while previously mentioned dihedral angle [$54.14(1)^\circ$] is considered to be the herringbone angle.

Furthermore, the terminal aminophenyl moieties of molecules are linked through C3—H3... π interactions [$3.600(3)$ Å], nearly along the crystallographic axes *c*. These interactions form a supramolecular staircase motif (Fig. 3), with the dihedral angle between two terminal aminophenyl moieties (staircase angle) of $72.03(1)^\circ$.

The Cambridge Structural Database [35] was searched for related derivatives containing uncoordinated 2-aminophenyl–phenylimino fragment in order to compare molecular and crystal peculiarities of the compound. The search resulted in 10 relevant hits summarized in Table 4. To gain an insight into substantial differences in a planarity of investigated molecule, we have compared the dihedral angles between benzene rings within database search results.

Schiff bases derived from aromatic diamines tend to be planar as in the crystal structure of compounds **2**, **3** and **5** (aldimines). The planarity can be altered by steric effects as in the case of ketimines **6–11** (**R4** = Ph), for example in the structure of compound **7** where aminophenyl moiety is inclined to phenylimino moiety by $65.83(6)^\circ$ [41]. A bulky substituent in **R7** position can also affect

Table 4
Selected geometric parameters (τ°) of database search for 2-aminophenyl–phenylimino compounds.



Compound no./reference	R1	R2	R3	R4	R5	R6	R7	τ ($^\circ$) ^a
1/This work	H	H	H	O–CH ₂	H	H	H	8.16(1)
2/Ref. [36]	H	H	H	NO ₂	H	H	H	5.2(1)
3/Ref. [37]	H	H	H	Cl	H	H	NO ₂	3.61(5)
4/Ref. [38]	H	H	H	Me ₂ N	H	H	COPh	42.73(6)
5/Ref. [39]	H	H	H	C=NPh	H	H	H	21.19(6)
6/Ref. [40]	Ph	OH	H	H	Cl	H	H	61.65(7)
7/Ref. [41]	Ph	OH	H	H	OMe	H	H	65.83 (6)
8/Ref. [42]	Ph	OH	H	OMe	H	H	H	53.16 (1)
9/Ref. [43]	Ph	OH	Cl	H	Cl	H	H	45.09 (1)
10/Ref. [44]	Ph	OH	H	H	Br	H	H	62.71 (1)
11/Ref. [45]	Ph	OH	H	H	H	H	H	58.40 (7)

^a Dihedral angle between benzene rings.

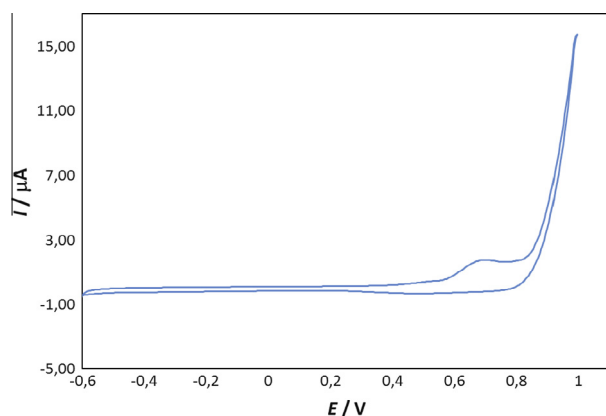


Fig. 4. Cyclic voltammogram of title compound ($c = 5.9 \times 10^{-4}$ mol dm⁻³) at a glassy carbon electrode ($l_c = 0.1$ M LiCl in DMF). Scan rate: $\nu = 100$ mV/s.

the planarity of aldimine compounds, as in compound **4** with angle of 47.23(6) $^\circ$. Recent studies of symmetrical bis-Schiff bases [2,46] have shown that the described deviation from planarity can affect spectral properties of material. It was found that the angle between benzene rings of the symmetrical bis-Schiff bases derived from 1,4-phenylenediamine [46] and 1,4-phthaldehyde [2] with different *p*-substituted anilines has an impact upon λ_{\max} of azomethine group.

It is very interesting to compare crystal packing of this work compound with compound **5** [35]. The compound **5** (N,N'-terephthalidenebis(o-aminoaniline)) has two polymorphic forms. One of the polymorphs crystallize in *P bca* space group and displays very similar packing motif as **1**. The molecules in crystal structure of **5** are also connected through the terminal amino groups and by a weak C–H $\cdots\pi$ interactions, thus stacking molecules into a simple herringbone motif. In addition, aminophenyl moieties of compound **5** are linked through the C–H $\cdots\pi$ interactions into a supramolecular staircase motif (Fig. S5). The herringbone angle in **5** is 65.20(1) $^\circ$ and dihedral angle between terminal aminophenyl moieties (staircase angle) is 71.93(6) $^\circ$. The bond geometry of C–H $\cdots\pi$ interaction [$d(D\cdots Cg) = 3.6181(1)$ and $\angle(DHCg) = 153^\circ$] between terminal aminophenyl moieties is almost identical as in **1**. The packing arrangement of molecules **1** and **5** (herringbone to staircase) is almost identical and most probably driven by the molecular

Table 5
Anodic peak potential ($E_{p,a}$) and anodic peak current ($I_{p,a}$) of the title compound ($c = 5.9 \times 10^{-4}$ mol dm⁻³) as the function of scan rate (ν).

ν (mV s ⁻¹)	$E_{p,a}$ (V)	$I_{p,a}$ (μ A)
25	0.670	0.924
75	0.677	1.087
100	0.679	2.120
200	0.697	2.283
250	0.702	2.500
300	0.707	2.848

structure of compounds (long, planar molecules) and by the absence of strong hydrogen bond donors and acceptors (e.g. OH).

Cyclic voltammetry studies

A cyclic voltammogram of the investigated Schiff base is shown in Fig. 4. Only one anodic peak is visible at a potential of 0.677 V when it was scanned from -0.6 V to 1.0 V vs. Ag/Ag⁺ reference electrode. The oxidation reaction involves the transfer of one electron which probably leads to the formation of a radical cation [47]. No reduction wave could be observed, indicating that the oxidation reaction is totally irreversible.

The influence of a scan rate on the oxidation of the Schiff base has been investigated and the results are shown in Table 5. The effect of concentration of the investigated Schiff base on anodic peak current and anodic peak potential was examined as well, and the obtained data are listed in Table 6. It can be seen from Tables 5 and 6, that both anodic peak potential and anodic peak current increase with the increase in Schiff base concentration and scan rate.

Table 6
Anodic peak potential ($E_{p,a}$) and anodic peak current ($I_{p,a}$) of the title compound as the function of its concentration. Scan rate: 100 mV/s.

$10^4 \times c$ (mol dm ⁻³)	$E_{p,a}$ (V)	$I_{p,a}$ (μ A)
0.5	0.579	0.532
1.9	0.599	0.696
2.8	0.618	1.304
4.5	0.646	1.848
5.9	0.679	2.120
6.1	0.689	2.337

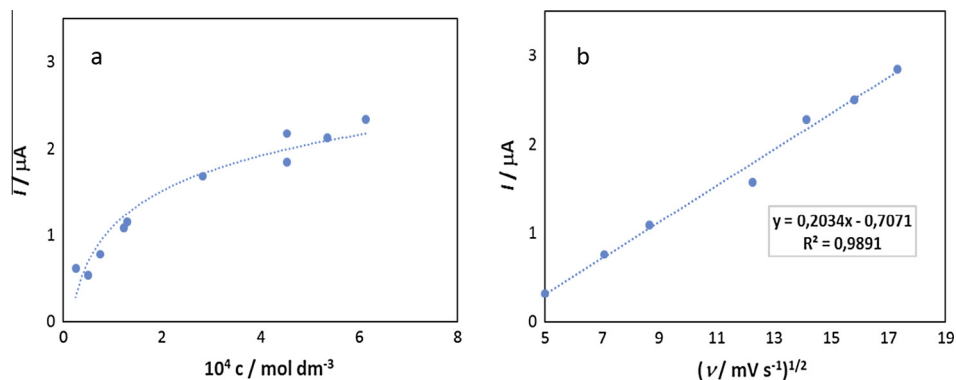


Fig. 5. (a) Anodic peak current as a function of title compound concentration ($I_c = 0.1$ M LiCl in DMF). Scan rate: 100 mV/s. (b) Anodic peak current, I , as a function of the square root of scan rate, $v^{1/2}$, at a glassy carbon electrode in solution of title compound ($c = 5.9 \times 10^{-4}$ mol dm $^{-3}$, $I_c = 0.1$ M LiCl in DMF).

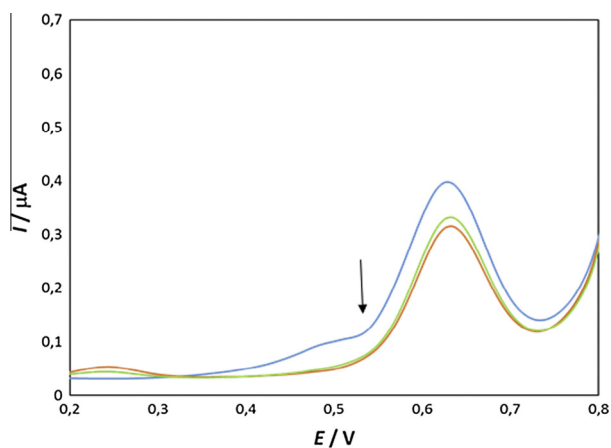


Fig. 6. Differential pulse voltammogram of title compound ($c = 5.9 \times 10^{-4}$ mol dm $^{-3}$) at a glassy carbon electrode ($I_c = 0.1$ M LiCl in DMF). Scan rate: 5 mV/s. First scan (—), second scan (—), third scan (—).

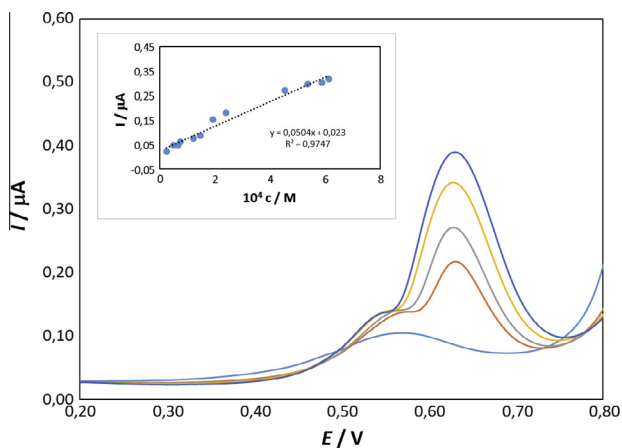


Fig. 7. Differential pulse voltammograms in the solutions of title compound ($c = 6.6 \times 10^{-5}$; 1.9×10^{-4} ; 2.8×10^{-4} ; 4.5×10^{-4} and 6.1×10^{-4} mol dm $^{-3}$) at a glassy carbon electrode ($I_c = 0.1$ M LiCl in DMF). Scan rate: 5 mV/s. Inset: Anodic peak current as a function of the title compound concentration ($I_c = 0.1$ M LiCl in DMF).

At lower concentration region (less than 1.3×10^{-4} mol dm $^{-3}$), anodic peak current is a linear function of the Schiff base concentration (Fig. 5a), which indicates that radical cation, oxidation product of the investigated compound, is adsorbed on the glassy

carbon electrode surface. At higher concentrations of Schiff base (above 1.3×10^{-4} mol dm $^{-3}$), peak current is leveling off, which could be explained by increasing interactions between molecules adsorbed on the glassy carbon electrode surface and interactions between oxidation product molecules which diffuse from bulk solution to working electrode surface and radical cation molecules adsorbed on the electrode surface [48,49]. It can also be seen from Fig. 5b that the Schiff base oxidation is controlled by diffusion since linear dependence was found between anodic peak current and the square root of scan rate [49,50].

Differential pulse voltammetry studies

Similarly to the above commented results, differential pulse voltammogram in Fig. 6 also reveals one oxidation peak of the investigated Schiff base at the potential of 0.630 V. The oxidation peak decreases with successive scans which confirms adsorption of the Schiff base oxidation product on the glassy carbon electrode surface. Due to the adsorption of the title compound oxidation product (radical cation) on the glassy carbon electrode surface, its concentration decreases in solution with successive scans, resulting in the decrease of oxidation peak current.

The results have shown that both oxidation peak current and oxidation peak potential are increasing with increase in Schiff base concentration (Fig. 7), as observed by cyclic voltammetry, which could be explained by kinetic limitation in the reaction between the redox sites of a glassy carbon electrode and the adsorbing product [51]. A linear relationship can be established between peak current and Schiff base concentration in the range from 0.25×10^{-4} mol dm $^{-3}$ to 6.10×10^{-4} mol dm $^{-3}$ (the inset of Fig. 7). A linear regression equation, $I_p = 0.0504c + 0.023$ with a correlation coefficient $R^2 = 0.9747$, can be obtained, where I_p is the oxidation peak current and c is the Schiff base concentration ($\times 10^{-4}$ mol dm $^{-3}$).

Conclusion

Novel symmetrical bis-Schiff base (1E)-1-N-[[4-(4-[[[(E)-N-(2-aminophenyl) carboxyimido] phenoxy]butoxy]phenyl)methylidene]benzene-1,2-diamine was synthesized in this study. The compound was characterized by means of single crystal X-ray analysis, spectroscopy (NMR and IR), elemental, TGA/DSC and electrochemical analysis. As it appears, the molecules are planar with small deviations of some functional groups and atoms from planarity. Such molecular shape is supported by strong intramolecular interactions. In the crystal, the molecules are arranged in a herringbone structural motif through the weak N—H...N and C—H... π interactions. Furthermore, the electrochemical results have shown

that the oxidation of the Schiff base compound is totally irreversible and diffusion controlled at the investigated experimental conditions. Adsorption of the oxidation product (radical cation) on the glassy carbon electrode occurs and this process is kinetically limited. A linear relationship between peak current and Schiff base concentration in the range of 0.25×10^{-4} mol dm⁻³ to 6.10×10^{-4} mol dm⁻³ was established.

Acknowledgements

We thank Prof. Dubravka Matković-Čalogović for single crystal data collection. Financial support for this research was provided by University of Osijek, Croatia.

Appendix A. Supplementary material

Supplementary data associated with this article can be found, in the online version, at <http://dx.doi.org/10.1016/j.molstruc.2014.12.009>.

References

- [1] C. Liang, J. Xia, D. Lei, X. Li, Q. Yao, J. Gao, *Eur. J. Med. Chem.* 74 (2014) 742–750.
- [2] Z. Fang, C. Cao, J. Chen, X. Deng, *J. Mol. Struct.* 1063 (2014) 307–312.
- [3] J. Zhao, B. Zhao, J. Liu, W. Xu, Z. Wang, *Spectrochim. Acta A* 57 (2001) 149–154.
- [4] V.I. Minkin, A.V. Tsukanov, A.D. Dubonosov, V.A. Bren, *J. Mol. Struct.* 998 (2011) 179–191.
- [5] S. Chandra, M. Pundir, *Spectrochim. Acta A* 69 (2008) 1–7.
- [6] P.A. Vigato, S. Tamburini, *Coord. Chem. Rev.* 248 (2004) 1717–2128.
- [7] S. Chattopadhyay, P. Chakraborty, M.G.B. Drew, A. Ghosh, *Inorg. Chim. Acta* 362 (2009) 502–508.
- [8] D. Maity, S. Chattopadhyay, A. Ghosh, M.G.B. Drew, G. Mukhopadhyay, *Polyhedron* 28 (2009) 812–818.
- [9] A. Iwan, H. Janeczka, B. Jarzabek, P. Rannou, *Materials* 2 (2009) 38–61.
- [10] A. Shanavas, S. Sathiyaraj, A. Chandramohan, T. Narasimhaswamy, A. Sultan, *J. Mol. Struct.* 1038 (2013) 126–133.
- [11] V. Cozan, M. Gaspar, E. Butuc, A. Stoleriu, *Eur. Polym. J.* 37 (2001) 1–8.
- [12] A. Iwan, P. Bilski, H. Janeczka, B. Jarzabek, M. Domanski, P. Rannou, A. Sikora, D. Pocięcha, B. Kaczmarczyk, *J. Mol. Struct.* 963 (2010) 175–182.
- [13] A. Iwan, D. Sek, *Prog. Polym. Sci.* 33 (2008) 289–345.
- [14] A.W. Jeevadason, K.K. Murugavel, M.A. Neelakantan, *Renew. Sustain. Energy Rev.* 36 (2014) 220–227.
- [15] J. Youn, S. Kewalramani, J.D. Emery, Y. Shi, S. Zhang, H.C. Chang, Y.J. Liang, C.M. Yeh, C.Y. Feng, H. Huang, C. Stern, L.H. Chen, J.C. Ho, M.C. Chen, M.J. Bedzyk, A. Facchetti, T.J. Marks, *Adv. Funct. Mater.* 23 (2013) 3850–3865.
- [16] J.E. Anthony, *Chem. Rev.* 106 (2006) 5028–5048.
- [17] A. Blagus, D. Cinčić, T. Friščić, B. Kaitner, V. Stilinović, *Chem. Eng.* 29 (2010) 117–138.
- [18] A. Blagus, B. Kaitner, *Acta Cryst. E* 67 (2011) o2908–o2909.
- [19] D. Işık, C. Santato, S. Barik, W.G. Skene, *Org. Electron* 13 (2012) 3022–3031.
- [20] M. Shakir, A. Abbasi, M. Azam, S.N. Khan, *Spectrochim. Acta A* 78 (2011) 29–35.
- [21] M. Shakir, A. Abbasi, M. Azam, A.U. Khan, *Spectrochim. Acta A* 79 (2011) 1866–1875.
- [22] T. Balić, B. Marković, I. Balić, *Acta Cryst. E* 69 (2013) o126.
- [23] STARe, Software 10.0, Mettler-Toledo GmbH, 2009.
- [24] CrysAlis PRO Oxford Diffraction Ltd, Yarnton, England.
- [25] M.C. Burla, R. Caliandro, M. Camalli, B. Carrozzini, G.L. Cascarano, L. DeCaro, C. Giacovazzo, G. Polidori, R. Spagna, *J. Appl. Cryst.* 38 (2005) 381–388.
- [26] L.J. Farrugia, *J. Appl. Crystallogr.* 32 (1999) 837.
- [27] G.M. Sheldrick, *Acta Cryst. A* 64 (2008) 112.
- [28] A.L. Spek, *Acta Cryst. A* 46 (1990) C34.
- [29] A.L. Spek, PLATON: A Multipurpose Crystallographic Tool, Utrecht University, Utrecht, The Netherlands, 1998.
- [30] C.F. Macrae, P.R. Edgington, P. McCabe, E. Pidcock, G.P. Shields, R. Taylor, M. Towler, J. Van der Streek, *J. Appl. Crystallogr.* 41 (2008) 466.
- [31] National Institute of Advanced Industrial Science and Technology. <<http://sdbs.riodb.aist.go.jp>>.
- [32] F.H. Allen, O. Kennard, D.G. Watson, L. Brammer, A.G. Orpen, R. Taylor, *J. Chem. Soc., Perkin Trans. 2* (1987) 1–19.
- [33] S.F. Kayed, Y.I. FarinaBaba, J. Simpson, *Acta Cryst. E* 64 (2008) o824–o825.
- [34] V.P. Singh, S. Singh, *Acta Cryst. E* 66 (2010) o1172.
- [35] F.H. Allen, *Acta Crystallogr. Sect. B* 58 (2002) 380.
- [36] B. Liu, W.Z. Lv, Z.K. Luo, X.L. Zhang, Y. Gao, J.H. Liu, *HuaxueShiji(Chin.)(Chemical Reagents)* 30 (2008) 434.
- [37] A.M. Farag, T.S. Guan, H. Osman, M.M. Rosli, H.K. Fun, *Acta Cryst. E* 66 (2010) o2220.
- [38] M.H. Habibi, M. Zendehehd, K. Barati, R.W. Harrington, W. Clegg, *Acta Cryst. E* 63 (2007) o2924.
- [39] L. Checinska, J. Lewkowski, M. Malecka, M. Dziegielewska, *J. Chem. Cryst.* 43 (2013) 421–428.
- [40] X.K. Ai, C.F. Bi, Y.H. Fan, X. Zhang, X.T. He, *Acta Cryst. E* 62 (2006) o3475.
- [41] K. Lippe, D. Gerlach, E. Kroke, J. Wagler, *Inorg. Chem. Commun.* 11 (2008) 492–496.
- [42] J. Wang, D. Cheng, L.D. Xuebao, *Zir.Kex.(Chin.)(J.Lanzhou.U.(Nat.Sci.))* 36 (2000) 61.
- [43] W.H. Li, F.Q. Liu, X.D. Zhao, J.Y. Deng, B.R. Hou, *Acta Cryst., E* 63 (2007) o3944.
- [44] Y. Xia, Q. Wang, J. You, *Acta Cryst. E* 63 (2007) o3529.
- [45] A. Blagus, B. Kaitner, *J. Chem. Cryst.* 37 (2007) 473–477.
- [46] Z. Fang, C. Cao, *J. Mol. Struct.* 1036 (2013) 447–451.
- [47] A. Aldenier, M.M. Chehimi, I. Gallardo, J. Pinson, *Langmuir* 20 (2004) 8243–8253.
- [48] B. Zeng, S. Wei, F. Xiao, F. Zhao, *Sens. Actuators, B* 115 (2006) 240–246.
- [49] M. Medvidović-Kosanović, M. Šeruga, L. Jakobek, I. Novak, *Collect. Czech. Chem. C* 75 (2010) 547–561.
- [50] A. Simić, D. Manojlović, D. Šegan, M. Todorović, *Molecules* 12 (2007) 2327–2340.
- [51] S. Menati, A. Azadbakht, A. Taeb, A. Kakanejadifard, H.R. Khavasi, *Spectrochim. Acta A* 97 (2012) 1033–1040.